44th AIAA Aerospace Sciences Meeting and Exhibit
9 - 12 January 2006, Reno, Nevada

AIAA 2006-602

# Nonlinear Control of Variable Speed Wind Turbines for Load Reduction and Power Optimization

B. Boukhezzar* and H. Siguerdidjane†
*Automatic Control Department, Supélec, Gif-sur-Yvette, F-91192 Cedex, France*
M. Hand‡
*National Renewable Energy Laboratory, Golden, CO, 80401, USA*

**To maximize wind power extraction, a variable speed wind turbine (VSWT) should operate as close as possible to its optimal power coefficient. The generator torque is used as a control input to improve wind energy capture by forcing the wind turbine (WT) to stay close to the maximum energy point. In general, current control techniques do not take into account the dynamical and stochastic aspect of both turbine and wind, leading to significant power losses. In addition, they are not robust with respect to disturbances. In order to address these weaknesses, a nonlinear approach, without wind speed measurement for VSWT control is proposed. Nonlinear static and dynamic state feedback controllers with wind speed estimator are then derived. The controllers were tested with a WT mathematical model, and are validated with an aeroelastic wind turbine simulator in presence of disturbances and measurement noise. The results have shown better performance in comparison with existing controllers.**

## Nomenclature

| | |
|---|---|
| $v$ | Wind speed, $\mathrm{m}\cdot\mathrm{s}^{-1}$ |
| $\rho$ | Air density, $\mathrm{kg}\cdot\mathrm{m}^{3}$ |
| $R$ | Rotor radius, m |
| $P_a$ | Aerodynamic power, W |
| $P_{a_{opt}}$ | Optimal aerodynamic power, W |
| $T_a$ | Aerodynamic torque, N·m |
| $\lambda$ | Tip speed ratio |
| $\beta$ | Pitch angle, deg |
| $\lambda_{opt}$ | Optimal tip speed ratio |
| $\beta_{opt}$ | Optimal pitch angle, deg |
| $C_p$ | Power coefficient |
| $C_q$ | Torque coefficient |
| $\omega_r$ | Rotor speed, $\mathrm{rad}\cdot\mathrm{s}^{-1}$ |
| $\omega_g$ | Generator speed, $\mathrm{rad}\cdot\mathrm{s}^{-1}$ |
| $T_{em}$ | Generator (electromagnetic) torque, N·m |
| $T_g$ | Generator torque in the rotor side, N·m |
| $T_{ls}$ | Low speed shaft torque, N·m |
| $T_{hs}$ | High speed shaft torque, N·m |
| $J_r$ | Rotor inertia, $\mathrm{kg}\cdot\mathrm{m}^2$. |
| $J_g$ | Generator inertia, $\mathrm{kg}\cdot\mathrm{m}^2$. |
| $J_t$ | Turbine total inertia, $\mathrm{kg}\cdot\mathrm{m}^2$. |
| $K_r$ | Rotor external damping, $\mathrm{N}\cdot\mathrm{m}\cdot\ \mathrm{rad}^{-1}\cdot$ s. |

*Automatic Control Department, boubekeur.boukhezzar@supelec.fr
†Automatic Control Department, houria.siguerdidjane@supelec.fr
‡Sr. Engineer, National Wind Technology Center, 1617 Cole Blvd./MS3811, ASME member

$K_g$ Generator external damping, N·m· rad$^{-1}$· s.
$K_t$ Turbine total external damping, N·m· rad$^{-1}$· s.
$K_{ls}$ Low speed shaft damping, N·m· rad$^{-1}$· s.
$B_{ls}$ Low speed shaft stiffness, N·m·rad$^{-1}$.
$n_g$ Gearbox ratio.
$P_a$ Aerodynamic power, W.
$P_e$ Electrical power, W.

# I. Introduction

VARIABLE-speed wind turbines have received a great deal of attention in recent years.[1] These turbines offer several advantages over constant-speed turbines. By operating over a broad range of wind speed, they are capable of greater energy capture. Structural loads can be reduced with variable-speed operation, and the significant power excursions common to constant-speed turbines are avoided. However, sophisticated control algorithms are necessary for variable-speed wind turbines to be profitable and reliable.
Variable-speed wind turbines operate in two primary regimes, below-rated power and above-rated power. When power production is below the rated power for the machine, the turbine operates at variable rotor speeds to capture the maximum amount of energy available in the wind. Generator torque provides the control input to vary the rotor speed, and the blade pitch angle is held constant. At rated power, the primary objective is maintaining constant, rated power output. This is generally achieved by holding the generator torque constant and varying the blade pitch angle. In both control regimes, the turbine response to transient loads must be minimized. This study focuses on control algorithms designed for the below-rated power operating regime.

Several wind turbine controllers have been proposed for the variable-speed operating regime. Ref.[2] defines the control objective as achieving optimal rotational speed tracking while rejecting fast wind speed variations and avoiding significant control efforts that induce undesirable torques and forces on the wind turbine structure. Several control strategies have been proposed in the literature primarily based on Linear Time-Invariant (LTI) models. Classical controllers have also been used extensively. Optimal control has been applied in the Linear Quadratic (LQ),[3,4] and Linear Quadratic Gaussian (LQG),[54] forms. Robust control was introduced in Ref.[6]-.[7] More recently, some non-linear control laws have been proposed,[8] and adaptive control has also been studied.[9] However, as mentioned in reference,[2] the drawbacks of these methods remain in the fact that nonlinear characteristics of the WT aerodynamics and structural behavior as well as the stochastic nature of the wind are not taken into consideration. In fact, by assuming the wind turbine operating in steady state conditions, the dynamic equations governing the WT behavior are not considered. Also, these papers assume that the WT operates on its optimal power curve to simplify the control laws synthesis. Because of the variability in the wind, the WT deviates significantly from the optimal power curve. Consequently the assumption of steady-state operation is not valid. Many of these investigations also required a measurement of the wind speed, which is generally obtained with a single anemometer. This single-point measurement does not adequately describe the full-field turbulent inflow that impinges upon the rotor. Also, this signal is generally averaged, but the control law is based upon an instantaneous value.

The objective of this paper is to demonstrate the feasibility of robust nonlinear controllers that take into consideration the dynamic aspect of the wind speed variation and the wind turbine response without need of wind speed measurements. The following section provides a brief description of WT model requirements. A simplified mathematical model is derived, and a complicated aeroelastic simulation is described. The control objectives of this work are specified, and existing control techniques are summarized. Section III describes the aerodynamic torque and wind speed estimator used in the proposed nonlinear state feedback controllers. The estimated aerodynamic torque and wind speed are obtained from noisy measurements of the rotor speed and the generator torque. The nonlinear feedback controllers are presented in Section IV. The dynamic state feedback controller with asymptotic rotor speed reference tracking combined with the estimator is shown to meet the required specifications in spite of the presence of a constant disturbance and measurement noise. Finally, Section V compares the performance results of the nonlinear feedback controllers with other controllers in the literature.

# II. Wind Turbine Modelling

## A. Model description

A wind turbine transforms part of the kinetic energy in the wind into electrical power. Wind turbine simulation complexity varies greatly depending upon the objectives of each one. Aeroelastic simulators are used to verify dynamic loads and interaction of the components of these large flexible structures. The combination of aerodynamic loading and dynamic response of multiple components requires complex simulators. Many efforts have been dedicated to the study of aeroelasticity and structural dynamics, and these efforts have produced wind turbine simulators that provide good predictions of loads and performance.
However, the complexity of such models is unnecessary for controller design. Consequently, simplified engineering models must be developed for control design. These models are simpler and easier to manage. They are generally described by a set of nonlinear ordinary differential equations that describe limited degrees of freedom of the wind turbine. The aerodynamic loads in these models are generally computed with semi-empirical models. These simplified fluid flow dynamics may lead to inaccurate results under certain conditions, particularly near and beyond stall. In this work, a simplified mathematical model is used for control law synthesis. Once the controllers are tested on this model, a complex aeroelastic simulator is used for validation of the controllers.

## B. System modelling

A variable-speed wind turbine generally consists of an aeroturbine, a gearbox, and a generator, as shown in Fig. 1). The aerodynamic power captured by the rotor is given by the non linear expression

$$P_a = \frac{1}{2}\rho\pi R^2 C_p(\lambda,\beta)v^3 \tag{1}$$

where $\omega_r$ is the rotor speed; $R$ is the rotor radius; and $\rho$ is the air density.
The power extracted from the wind, $P_a$, is proportional to the cube of the wind speed $v$. The power coefficient, $C_p$, depends on the blade pitch angle, $\beta$, and the tip-speed ratio, $\lambda$, which is defined as the ratio between the linear blade tip speed and the wind speed $v$.

$$\lambda = \frac{\omega_r R}{v} \tag{2}$$

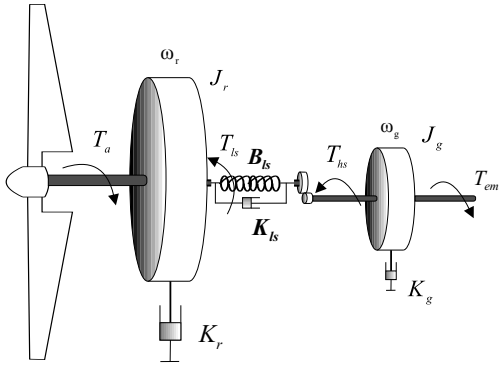


**Figure 1. Wind turbine dynamics.**

Thus, any change in the rotor speed or the wind speed induces change in the tip-speed ratio leading to power coefficient variation. In this way, the generated power is affected. The aerodynamic torque coefficient is related to the power coefficient as follows. Using the relationship.

$$P_a = \omega_r T_a \tag{3}$$

the aerodynamic torque expression is then

$$T_a = \frac{1}{2}\rho\pi R^3 C_q(\lambda,\beta)v^2 \tag{4}$$

where

$$C_q(\lambda,\beta) = \frac{C_p(\lambda,\beta)}{\lambda}$$

Power and torque coefficient surfaces for the wind turbine considered in this study are shown in Figure 2. These surfaces are obtained using blade-element moment theory implemented in a wind turbine performance code, WT-PERF,[10] developed by NREL. These surfaces are implemented in the mathematical model as look-up tables.
The dynamic response of the rotor driven at a speed $\omega_r$ by the aerodynamic torque $T_a$ is shown to be

$$J_r\dot{\omega}_r = T_a - T_{ls} - K_r\omega_r \tag{5}$$

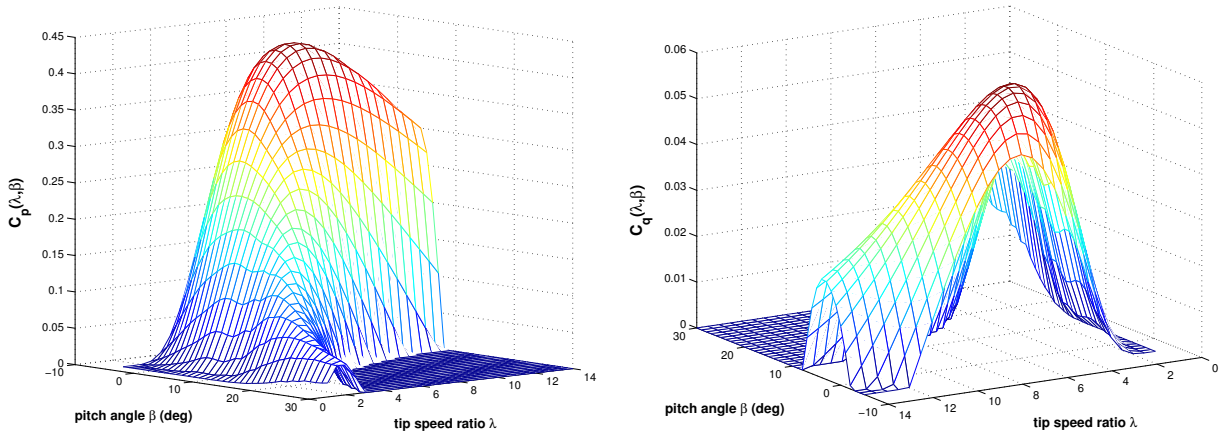


(a) $C_p(\lambda, \beta)$ curve.

(b) $C_q(\lambda, \beta)$ curve.

**Figure 2. Aerodynamic power and torque coefficients curves.**

The low-speed shaft torque $T_{ls}$ acts as braking torque on the rotor (See Figure 1). It results from the torsion and friction effects due to the difference between $\omega_r$ and $\omega_{ls}$

$$T_{ls} = B_{ls}(\theta_r - \theta_{ls}) + K_{ls}(\omega_r - \omega_{ls}) \tag{6}$$

The generator is driven by the high speed shaft torque $T_{hs}$ and braked by the generator electromagnetic torque $T_{em}$.

$$J_g \dot{\omega}_g = T_{hs} - K_g \omega_g - T_{em} \tag{7}$$

Assuming an ideal gearbox with transmission ratio $n_g$, we have

$$n_g = \frac{T_{ls}}{T_{hs}} = \frac{\omega_g}{\omega_{ls}} \tag{8}$$

Transferring the generator dynamics to the low speed side and using Eq. (7) and Eq. (8), the generator dynamics can be written as

$$n_g^2 J_g \dot{\omega}_g = T_{ls} - (n_g^2 K_g)\omega_g - n_g T_{em} \tag{9}$$

If a perfectly rigid low-speed shaft is assumed, a single mass model of the turbine may then be considered

$$J_t \dot{\omega}_r = T_a - K_t \omega_r - T_g \tag{10}$$

where

$$\begin{aligned} J_t &= J_r + n_g^2 J_g \\ K_t &= K_r + n_g^2 K_g \\ T_g &= n_g T_{em} \end{aligned}$$

### C. Simulator description

The Fatigue, Aerodynamics, Structures and Turbulence (FAST) code developed by NREL is an aeroelastic WT simulator that is capable of modeling two- and three-bladed propeller-type machines. This code is used by WT designers to predict both extreme and fatigue loads. It uses an assumed mode method to model flexible blades and tower components. Other components are modelled as rigid bodies. Because this study focused on low wind conditions, flexibility in the tower and blades were neglected. In this study, three degrees-of-freedom (DOFs) are simulated: the variable generator and rotor speed (2 DOFs) and the blade teeter DOF. The variable generator and rotor speed DOFs account for the variations in generator speed and the drive train flexibility associated with torsional motion between the generator and hub/rotor. The blade teetering DOF accounts for the teeter motion induced by asymmetric wind loads across the rotor plane.

### D. Control objectives

The $C_p(\lambda, \beta)$ curve in Eq. (1) is specific for each wind turbine. It has a unique maximum $C_{p_{opt}}$ at a single point

$$C_p(\lambda_{opt}, \beta_{opt}) = C_{p_{opt}} \tag{11}$$

that corresponds to maximum power production in below-rated power conditions. To maximize wind power extraction, the blade pitch angle, $\beta$, is fixed to the optimal value, $\beta_{opt}$, and the WT should continuously operate at the optimal tip-speed ratio, $\lambda_{opt}$. For a given wind speed, $v$, in order to maintain $\lambda$ at its optimal value, the rotor speed must be adjusted using generator torque to track the reference $\omega_{r_{opt}}$ that has the same shape as wind speed, since they are proportional.

$$\omega_{r_{opt}} = \frac{\lambda_{opt}}{R} v \tag{12}$$

Hence, in the partial load area, the WT is a single-input, single-output (SISO) system. The control input is the generator torque referenced to the low-speed side of the gearbox. The system output to be controlled is the rotor speed, $\omega_r$, and the control problem is the tracking of an optimal rotor speed reference, $\omega_{r_{opt}}$, that ensures maximum wind power capture.

### E. Baseline control strategies

In order to make a comparison between the proposed controllers and existing controllers, a brief description of two well-known control techniques is given here. In Ref.,[11] an Aerodynamic Torque Feed Forward (ATF) controller is described. The aerodynamic torque and the rotor speed are estimated using a Kalman Filter. The estimated aerodynamic torque is fed into the generator reference torque. Ref.[11] mentions that since the tracked wind speed constantly changes, there is no need for eliminating the steady-state error with an integral term in the control law. Therefore a proportional control law is used.

$$T_g = K_c(\omega_{ref} - \hat{\omega}_r) + \hat{T}_a - K_t \hat{\omega}_r \tag{13}$$

where

$$\omega_{ref} = \sqrt{\frac{\hat{T}_a}{k_{opt}}} \tag{14}$$

with

$$k_{opt} = \frac{\rho}{2} \pi R^5 C_{p_{opt}} \frac{1}{\lambda_{opt}^3}$$

The control scheme is shown in Figure 3.

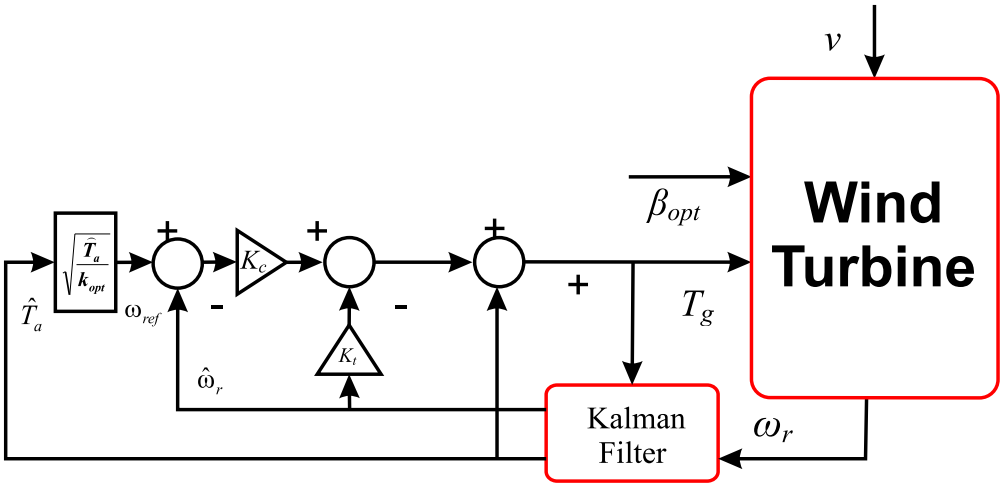


**Figure 3. ATF control scheme.**

In duplicating the ATF model for this study, during simulation with a wind speed step, we find that a steady state error remains particularly in the presence of disturbances. The values of $k_{opt}$ and $C_{p_{opt}}$ are generally obtained by the control engineer from performance models such as those used to determine the surfaces in Fig. 2. Since $k_{opt}$ is proportional to $C_{p_{opt}}$, when the simulated value of $k_{opt}$ is different from the turbine's actual one, steady-state operation will occur at a value of $C_{p_{opt}}$ that is not the real system's best operating point.[12] The problem with uncertainty of $C_{p_{opt}}$ has not been considered in this work. However, it becomes important for experimentation on real machines. An additional drawback of this technique is the assumption that the WT operates close to the optimal rotor speed, $\omega_{ref}$, which is obtained by setting $T_a = T_{a_{opt}}$. The difference between $\omega_{r_{opt}}$ and $\omega_{ref}$ induces significant power losses during the transitions. Therefore, a more precise value of $\omega_{ref}$ is needed.
Ref[13] shows that a wind turbine is locally stable to any equilibrium operating point on the optimal aerodynamic efficiency curve. One can maintain $T_a$ on this curve by choosing a control torque $T_g$ that tracks the same value rather than tracking wind speed variations

$$T_g = k_{opt}\omega_r^2 - K_t\omega_r \tag{15}$$

This method is known as the Indirect Speed Control (ISC) technique. Fig. 4 shows the ISC control scheme. In constant wind speeds, the ISC controller will achieve the tip-speed ratio for optimum operation. However in varying wind, the inertia of the rotor prevents continuous operation at $C_{p_{opt}}$.[14] Nevertheless, the transitions during fast wind speed variations result in power losses. Additionally, the control strategy is not robust with respect to measurement noise and disturbances.

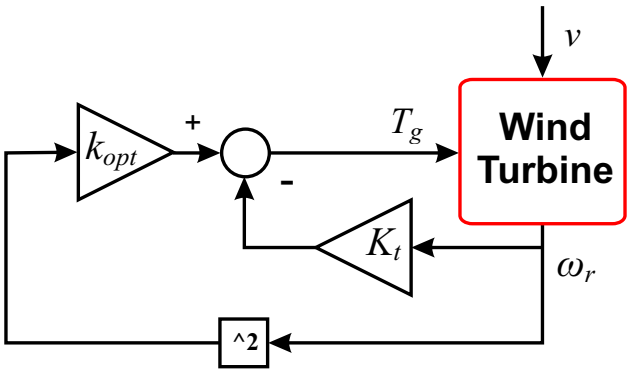


**Figure 4. ISC control scheme.**

In summary, the control techniques described above show two main drawbacks: on the one hand, they do not take into consideration the dynamic aspect of the wind and the turbine; on the other hand, they are not robust with respect to measurement noise and disturbances. In order to address these weaknesses, a nonlinear dynamic state feedback controller with a wind speed estimator will be presented. Furthermore, this structure allows the rejection of disturbances acting on the control torque $T_g$.

## III. Estimation of wind speed and aerodynamic torque

The wind speed, $v$, that appears in the aerodynamic torque and power expression of Eq. (1) and Eq. (4) is actually a kind of spatial average of the three-dimensional wind field that impinges upon the rotor blades. The wind speed field varies over the disc swept by the rotor,[15] it is then impossible to represent this one by a unique measure. In practice, the wind speed measured by an anemometer does not represent the effective wind speed $v$. The rotor effective wind speed is defined as a single point wind speed signal which will cause torque variations through thrust and torque coefficients that will be stochastically equivalent to those calculated with blade element theory in a turbulent wind field.[16] Aiming to obtain a more representative value of $v$ and to control the wind turbine without using an anemometer signal, we use the wind turbine as a measurement device. We do this in two steps: estimation of the aerodynamic torque and deduction of the wind speed.

### A. Aerodynamic torque estimation

A Kalman filter is used to estimate aerodynamic torque $T_a$ by appending it as an additional state. The dynamics for this state are driven by white noise

$$\begin{aligned} \begin{bmatrix} \dot{\omega_r} \\ \dot{T_a} \end{bmatrix} &= \begin{bmatrix} -\frac{K_t}{J_t} & \frac{1}{J_t} \\ 0 & 0 \end{bmatrix} \begin{bmatrix} \omega_r \\ T_a \end{bmatrix} + \begin{bmatrix} -\frac{1}{J_t} \\ 0 \end{bmatrix} T_g + \begin{bmatrix} 0 \\ 1 \end{bmatrix} \xi \\ y &= \omega_r + \zeta \end{aligned} \tag{16}$$

$\xi$ is the process noise and $\zeta$ the measurement noise. They are a centered white, non correlated, Gaussian noise. Ref.[17] proves that if the state noise variance is non-zero, the Kalman estimator corresponding to the system in Eq. (16) is convergent. In this Kalman filter approach, the estimated state is not exploited to deduce the optimal reference speed $\omega_{r_{opt}}$. Rather, the estimated state $\left[\hat{\omega_r}\ ,\ \hat{T_a}\right]^t$ is used to obtain an estimate of the effective wind speed, $\hat{v}$, from which the optimal rotor speed is derived. Moreover, as the rotor speed measurement is disturbed, it is preferable to use its estimate in the control laws.

### B. Wind speed estimation

The aerodynamic torque depends nonlinearly on the rotor speed $\omega_r$ and also on the wind speed $v$. The effective wind speed $v$ is related to $T_a$ through the expression for aerodynamic torque when the pitch angle is held at its optimal value.

$$T_a = \frac{1}{2}\rho\pi R^3 C_q(\lambda) v^2 \tag{17}$$

where

$$C_q(\lambda) = C_q(\lambda, \beta_{opt})$$

Using Eq. (17) and the estimated aerodynamic torque and rotor speed obtained in Eq. (16), the estimate of wind speed, $\hat{v}$, is found by solving the following algebraic equation.

$$\hat{T}_a - \frac{1}{2}\rho\pi R^3 C_q\left(\frac{\hat{\omega_r} R}{\hat{v}}\right)\hat{v}^2 = 0 \tag{18}$$

In order to use numerical algorithms for solving Eq. (18), an analytic expression of $C_q(\lambda)$ is needed. Because it is given through a look-up table, $C_q$ is approximated by a polynomial in $\lambda$.

$$C_q(\lambda) = \sum_{i=0}^{n} a_i \lambda^i$$

Eq. (18) is finally solved using the Newton algorithm. Because this equation has a unique solution in the below rated power operating regime, the convergence of the algorithms is achieved after only a few iterations. Having $\hat{v}$, the estimated optimal rotor speed, $\hat{\omega}_{r_{opt}}$ is thus

$$\hat{\omega}_{r_{opt}} = \frac{\lambda_{opt}\hat{v}}{R} \tag{19}$$

It is important to note that estimation of $\omega_{r_{opt}}$ does require a good estimate of the wind speed. This estimator is then used to design nonlinear control laws for optimal rotor speed tracking of $\omega_{r_{opt}}$ to improve the aerodynamic efficiency while reducing the drive train transient loads.

## IV. Nonlinear State Feedback Control with Estimator

### A. Nonlinear static state feedback control with estimator

The nonlinear behavior of the WT described by Eq. (10) is linearized using the aerodynamic torque estimate $\hat{T}_a$.
By imposing the following control torque,

$$T_g = J_t\left[\frac{\hat{T}_a}{J_t} - \frac{K_t}{J_t}\omega_r - w\right] \tag{20}$$

$w$ is the new input of the linearized system. Eq. (10) simplifies to

$$\dot{\omega}_r = w \tag{21}$$

A first order dynamic response is selected for the rotor speed tracking error $\hat{\varepsilon}$.

$$\dot{\hat{\varepsilon}} + a_0\hat{\varepsilon} = 0 \tag{22}$$

where

$$\hat{\varepsilon} = \hat{\omega}_{opt} - \hat{\omega}_r \tag{23}$$

From Eq. (21) and (22), the new input $w$ is obtained

$$w = \dot{\hat{\omega}}_{r_{opt}} + a_0(\hat{\omega}_{r_{opt}} - \hat{\omega}_r) \tag{24}$$

By substituting Eq. (24) of $w$ in (20), the generator torque $T_g$ is thus

$$T_g = \hat{T}_a - K_t\hat{\omega}_r - J_t a_0\hat{\varepsilon} - J_t\dot{\hat{\omega}}_{t_{opt}} \tag{25}$$

This technique has been shown to lack robustness with respect to perturbations,[18] so a nonlinear dynamic state feedback controller is developed next.

### B. Nonlinear dynamic state feedback control with estimator

Higher order dynamic response of the tracking error can be imposed to produce a dynamic state feedback controller. Assuming a constant disturbance $d$ acting on the wind turbine, Eq. (10) becomes

$$J_t\dot{\omega}_r = T_a - K_t\omega_r - T_g + d \tag{26}$$

The disturbance may represent an unmodeled or unknown phenomenon which affects the WT behavior, e.g. solid friction. Taking the time derivative of Eq. (26), we get

$$J_t\ddot{\omega}_r = \dot{T}_a - K_t\dot{\omega}_r - \dot{T}_g \tag{27}$$

As in the nonlinear static state feedback controller, the control torque

$$\dot{T}_g = \frac{1}{J_t}\left[\frac{\dot{\hat{T}}_a}{J_t} - \frac{K_t}{J_t}\dot{\hat{\omega}}_r - w\right] \tag{28}$$

results in a linear system with a new input, $w$. Substituting Eq. (28) into Eq. (10) results in

$$\ddot{\omega}_r = w \tag{29}$$

We now choose a second order differential equation to govern the tracking error $\hat{\varepsilon}$

$$\ddot{\hat{\varepsilon}} + b_1\dot{\hat{\varepsilon}} + b_0\hat{\varepsilon} = 0 \tag{30}$$

Substituting Eqs. (23) and (29) into Eq. (30) produces

$$w = \ddot{\hat{\omega}}_{r_{opt}} + b_1(\dot{\hat{\omega}}_{r_{opt}} - \dot{\hat{\omega}}_r) + b_0(\hat{\omega}_{r_{opt}} - \hat{\omega}_r) \tag{31}$$

and finally the generator torque dynamics are given by

$$\dot{T}_g = \dot{\hat{T}}_a - K_t\dot{\hat{\omega}}_r - J_t\ddot{\hat{\omega}}_{opt} - J_t b_1\dot{\hat{\varepsilon}} - J_t b_0\hat{\varepsilon} \tag{32}$$

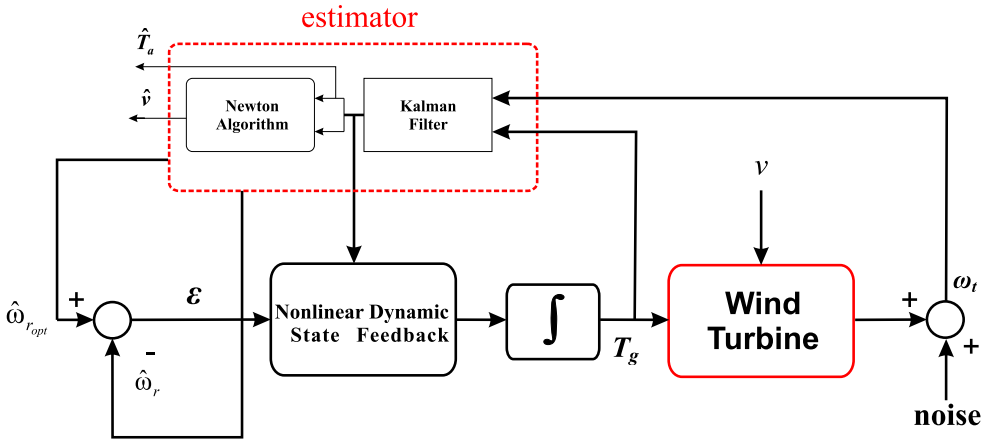


**Figure 5. Nonlinear dynamic state feedback with estimator controller scheme.**

A diagram of the dynamic state feedback controller with wind speed estimator is shown in Fig. 5. All the time derivatives that appear in the generator torque expressions, Eq. (25) and (32) are obtained using approximated filtered derivatives. Very fast dynamics will lead to wind speed turbulence tracking, but large control loads will also occur. So the dynamic response must be designed to track the average wind speed over short time intervals. This decreases the rapid variations in generator torque, which is beneficial. Very quick changes in $T_g$ are not desirable.

## V. VALIDATION RESULTS

The numerical simulations were performed on a wind turbine whose characteristics are given in Table 1. These parameters correspond to the Controls Advanced Research Turbine (CART) which is located at NREL's National Wind Technology Center near Boulder, CO. The CART is a variable-speed, variable pitch WT with a nominal power rating of 600 kW and a hub height of 36 m. It is a 43-m diameter, 2-bladed, teetered hub machine. The gearbox is connected to an induction generator via the high-speed shaft, and the generator is connected to the grid via power electronics. This turbine was modelled with the mathematical model and the FAST aeroelastic simulator for comparison.

The wind inflow for the simulations consists of one 10-minute data set of full-field turbulent wind. Fig. 6 illustrates the hub-height wind speed variation. This turbulent wind data was generated using the Class A Kaimal turbulence spectra. It has a mean value of 7 m/s at the hub height and a turbulence intensity of 25 %. Using this excitation, each of the four controllers discussed are compared for energy capture and transient load reduction.

As mentioned in Section II.D, the control objective is to maximize the captured energy from the wind while limiting the transient loads experienced by the turbine. For this study, the low-speed shaft torsion was minimized, which is equivalent to reducing the variance of the high-speed shaft torsional moment. The constraints on the generator torque and the rotor speed of 162 kN.m and 58 rpm, respectively, were also observed.

**Table 1. Wind turbine characteristics**

| | |
|---|---|
| Rotor diameter | 43.3 m |
| gearbox ratio | 43.165 |
| Hub height | 36.6 m |
| Generator system electrical power | 600 kW |
| Maximum rotor torque | 162 KN.m |

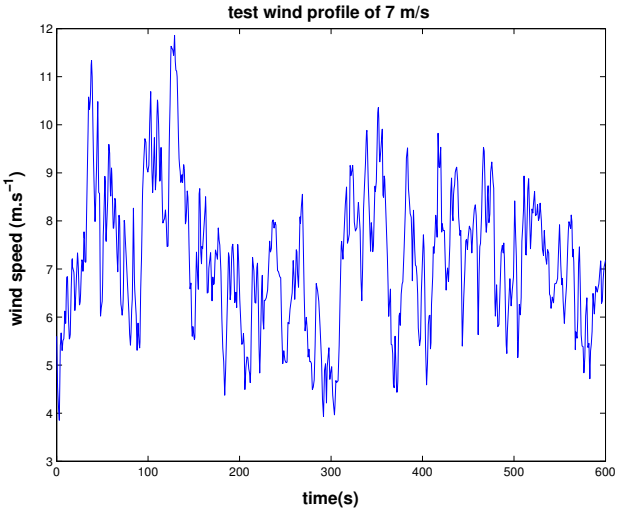


**Figure 6. Wind speed profile of 7 $\mathrm{m.s^{-1}}$ mean value.**

### A. Using the mathematical model

First, the performance of the nonlinear dynamic state feedback controller (32) is verified using the mathematical model. An additive measurement noise on $\omega_r$ has been introduced. This is a band-limited, white noise obtained by using a normally distributed random number generator in series with a zero-order hold. This method approximates an ideal centered white Gaussian noise. The Signal to Noise Ratio (SNR) is approximately 7 dB. In addition, a constant, additive disturbance $d$ of 10 kN.m on the control torque $T_g$ has also been introduced.
Fig. 7(a) shows that the rotor speed $\omega_r$ tracks the mean tendency of the optimal rotational speed $\omega_{r_{opt}}$ without tracking the turbulent component. The difference between the rotor speed and its optimal reference is most evident during the start-up transient. Fig. 8(a) shows acceptable control loads where the commanded torque does not exceed the design maximum of 162 kN.m. The generator torque remains smooth and induces low frequency variations in the generator currents. These are good conditions for electrical devices.

### B. Validation using FAST

The nonlinear dynamic state feedback controller was implemented using the FAST wind turbine dynamic simulation. Fig. 7(b) shows that the rotor speed variations remain smooth while tracking the mean tendency of the optimal rotational speed. Similarly to the mathematical model, the differences between the optimal rotor speed reference and rotor speed occur during the start-up transient. Although the generator torque from the FAST model (Fig. 8(b)) is greater than that obtained with the mathematical model, it remains below the maximum acceptable value. The nonlinear dynamic state feedback controller with estimator (NDSFE) ensures the rejection of the disturbance on the control torque. The Kalman filter used with the Newton algorithm provides a good estimate of the wind speed through the aerodynamic torque estimate and rotor speed estimate even with the noisy measurements of $\omega_r$ and $T_g$.
Fig. 10-12 compare the performance obtained using the nonlinear static and the nonlinear dynamic state feedback controllers. In Fig. 10, the nonlinear static state feedback controller (25) is unable to reject the unknown disturbance applied to the control input. This is the source of the deviation of the rotor speed from its optimal reference between 300 and 400 s. Conversely, the nonlinear dynamic state feedback controller (32) succeeded in keeping the rotor speed in the neighborhood of the optimal reference speed in spite of the presence of the disturbance. Fig. 11 shows the additional control torque demanded by the NDSFE controller to reject the additive disturbance. The control torque still remains below the upper bound, though. Fig. 12 shows that this disturbance rejection results in increased energy capture for the NDSFE controller as compared to the nonlinear static state feedback controller.

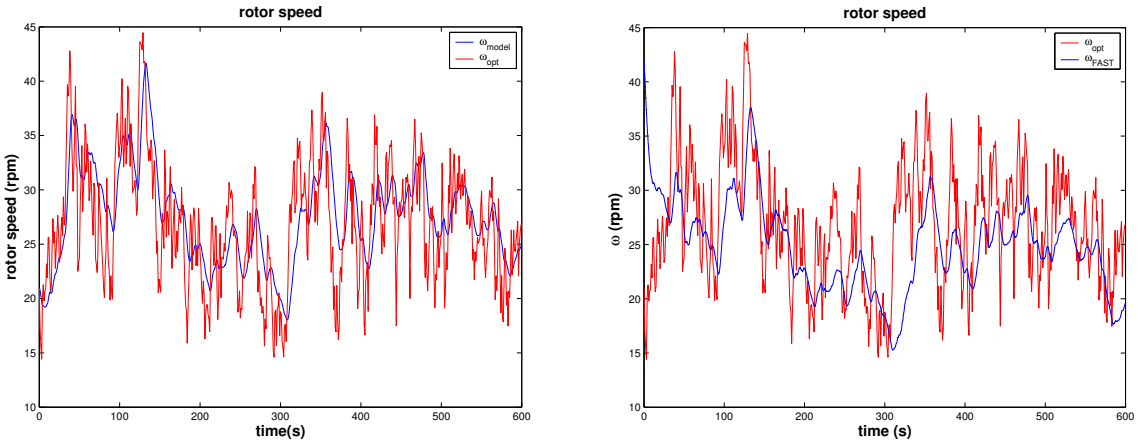


(a) Mathematical model (b) FAST simulator

**Figure 7. Nonlinear dynamic state feedback control, with estimator: Rotor speed responses**

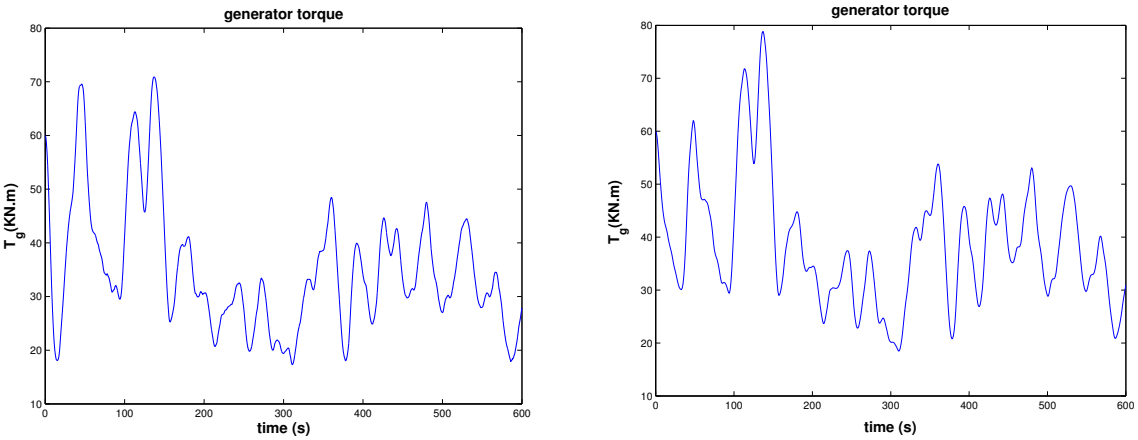


(a) Mathematical model (b) FAST simulator

**Figure 8. Nonlinear dynamic state feedback control, with estimator: Generator torque responses**

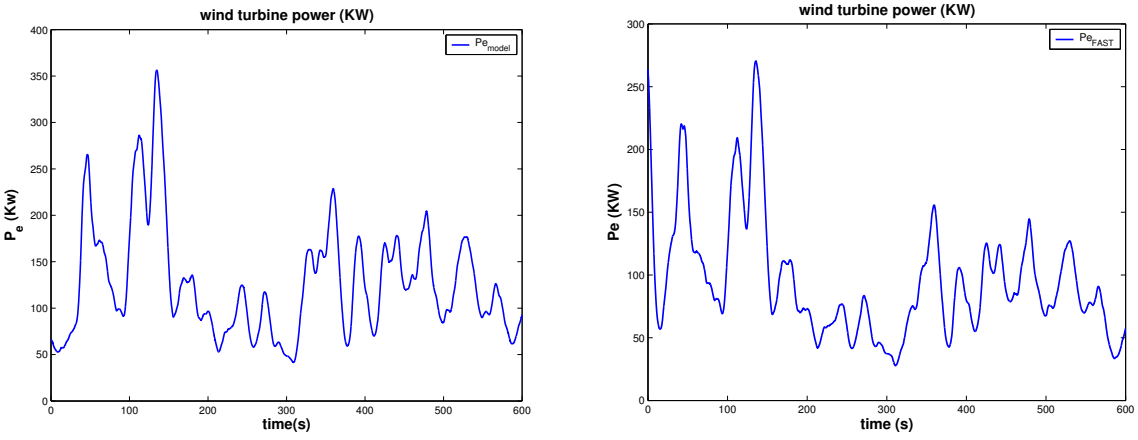


(a) Mathematical model (b) FAST simulator

**Figure 9. Nonlinear dynamic state feedback controller, with estimator: Wind turbine power**

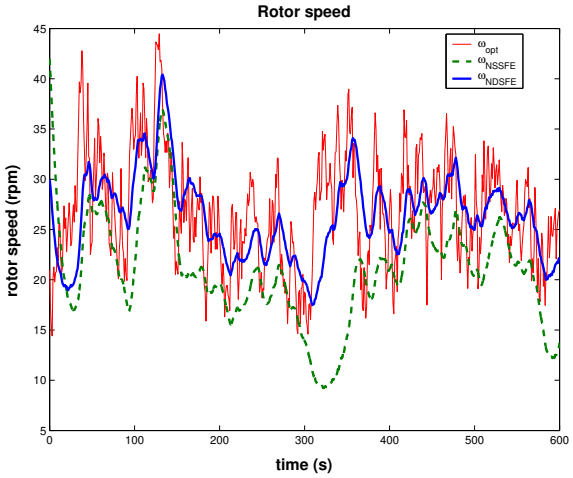


**Figure 10. Nonlinear static and dynamic state feedback controller, with estimator: Rotor speed responses with FAST**

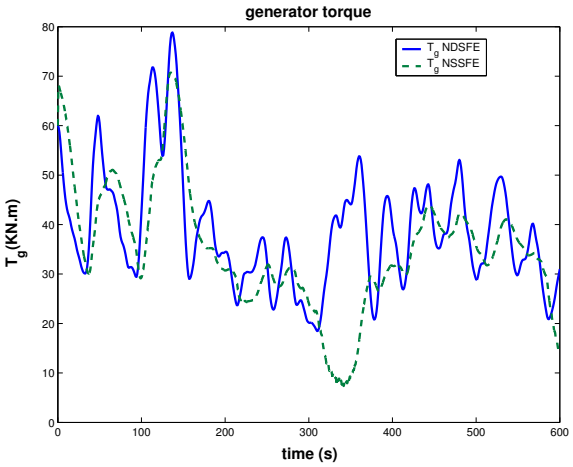


**Figure 11. Nonlinear static and dynamic state feedback controller, with estimator: Generator torque responses with FAST**

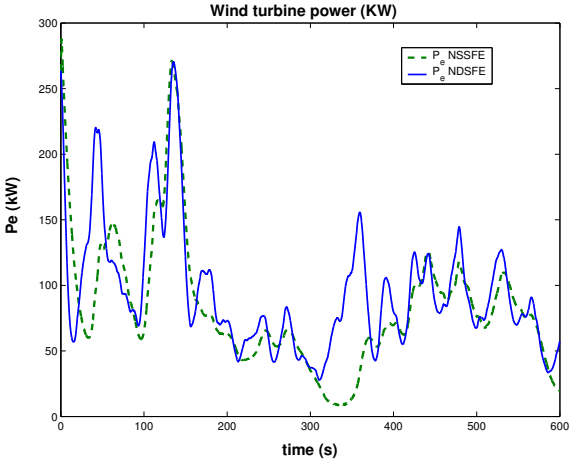


**Figure 12. Nonlinear static and dynamic state feedback controller, with estimator: Wind turbine power with FAST**

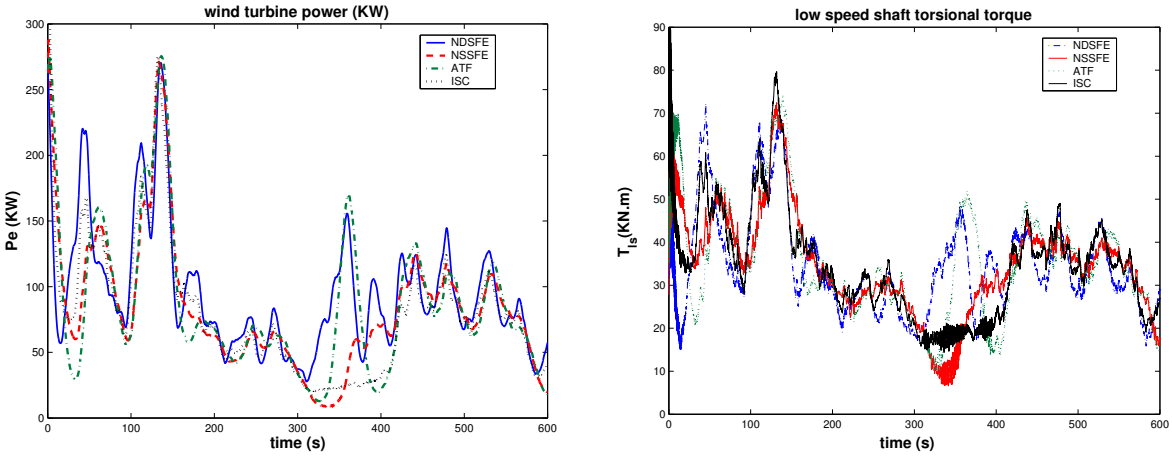


(a) electrical power

(b) low speed shaft torque

**Figure 13. Electrical power and low speed shaft torque using the different control strategies**

These new controllers are compared with the two baseline controllers described in Section E. The simulations were conducted with the FAST model with the same operating conditions, disturbance, and measurement noise. The performance differences are illustrated in Fig. 13 and tabulated in Table 2. The power capture efficiency is defined as the ratio between the energy captured during the simulation and the maximum amount of energy available if the turbine could operate at its optimal power coefficient.

$$\text{Efficiency} = \frac{\int_{t_{ini}}^{t_{fin}} P_e dt}{\int_{t_{ini}}^{t_{fin}} P_{a_{opt}} dt} \tag{33}$$

where

$$P_{a_{opt}} = \frac{1}{2}\rho\pi R^2 C_{p_{opt}} v^3 \tag{34}$$

and $P_e$ is the electrical power. Fig. 13(a) shows that the produced electric power using the NDSFE controller is greater than that of the other controllers. In the time interval from 300 to 400 s the effect of the disturbance is evident. The ISC, NSSFE, and ATF controllers do not reject the disturbance and therefore power is lost. However, the NDSFE controller does reject the disturbance capturing energy during this period. The low-speed shaft torque oscillations tend to be reduced during this period for the NDSFE controller as shown in Fig. 13(b). The NDSFE controller achieves a 10 % increase in efficiency over the ISC controller with a decrease of 1.14 kN.m on the standard deviation of the low-speed shaft torque.

**Table 2. Comparison of the different control strategies**

| | Efficiency [%] | $T_{hs}$ standard deviation [kN.m] | $\max(T_g)$ [kN.m] |
|---|---|---|---|
| ISC | 51.79 | 12.73 | 112.34 |
| NSSFE | 61.23 | 11.87 | 70.70 |
| ATF | 63.43 | 13.19 | 76.99 |
| NDSFE | 69.96 | 11.59 | 70.90 |

# VI. CONCLUSION

For a variable-speed wind turbine, the primary control objective below rated power is to extract the maximum amount of energy from the wind. The control authority, however, must not exceed design constraints and must not introduce excessive transient loads. Many existing control techniques assume the wind and the turbine operate in steady-state conditions. Consequently, significant power losses occur due to wind speed variability. Controllers based on nonlinear static and dynamic state feedback linearization with asymptotic rotor speed reference tracking were proposed. With the aim of accounting for the wind turbine nonlinear aerodynamic characteristics as well as the stochastic nature of the wind, an aerodynamic torque and wind speed estimator was developed. These controllers were compared to standard controllers using an aeroelastic wind turbine simulator. The nonlinear dynamic state feedback with estimator controller demonstrated the ability to reject a disturbance and operate with measurement noise. In so doing, this controller extracted more power than the other controllers. This study has produced satisfactory results demonstrating the efficiency improvement capability of the new controllers.

# References


[1]Burton, T., Sharpe, D., Jenkins, N., and Bossanyi, E., *Wind Energy Handbook*, John Wiley & Sons, 2001.

[2]Boukhezzar, B. and Siguerdidjane, H., "Robust Multiobjective Control of a Variable Speed Wind Turbine," *European Wind Energy Conference Proceedings*, EWEA, London, UK, 2004.

[3]Abdin, E. S. and Xu, W., "Control Design and Dynamic Performance Analysis of a Wind Turbine-Induction Generator Unit," *IEEE Transactions on energy conversion*, Vol. 15, No. 1, 2000, pp. 91–96.

[4]Ekelund, T., *Modeling and Linear Quadratic Optimal Control of Wind Turbines*, Ph.D. thesis, Chalmers University of Technology, Sweden, 1997.

[5]Connor, B., Leithead, W. E., and Grimble, M., "LQG control of a constant speed horizontal axis wind turbine," *Proceedings of the Third IEEE Conference on Control Applications*, Vol. 1, 1994, pp. 251–252.

[6]Bongers, P., *Modeling and identification of flexible wind turbines and a factorizational approach to robust control*, Ph.D. thesis, Delft University of Technology, Netherlands, 1994.

[7]Connor, D., Iyer, S. N., Leithead, W. E., and Grimble, M. J., "Control of horizontal axis wind turbine using $H_\infty$ control," *Proceedings of the First IEEE Conference on Control Applications*, 1992.

[8]Battista, H. D., Mantz, R. J., and Christiansen, C. F., "Dynamical Sliding Mode Power Control of Wind Driven Induction Generators," *IEEE Transactions on energy conversion*, Vol. 15, No. 14, 2000, pp. 451–457.

[9]Y. D. Song, B. D. and Bao, X. Y., "Variable speed control of wind turbines using nonlinear and adaptive algorithms," *Journal of Wind Engineering and Industrial Aerodynamics*, Vol. 85, 2000, pp. 293–308.

[10]Buhl, M. L., "WT_PERF USER'S GUIDE," Tech. rep., National Renewable Energy Laboratory, Golden, Colorado, 2004.

[11]Vihriälä, H., Perälä, R., Mäkilä, P., and Söderlund, L., "A gearless wind power drive: Part 2: Performance of control system," *Proceedings of the European Wind Energy Conference*, 2001.

[12]Johnson, K. E., "Adaptive Torque Control of Variable Speed Wind Turbines," NREL Report NREL/TP-500-36265, National Renewable Energy Laboratory, Golden, Colorado, Aug. 2004.

[13]Leithead, W. E. and Connor, D., "Control of Variable Speed Wind Turbines: Design Task," *International Journal of Control*, Vol. 73, 2000, pp. 1173–1188.

[14]Pierce, K., "Control Method for Improved Energy Capture below Rated Power," *Proceedings of the* $3^{rd}$ *ASME/JSME Joint Fluids Engineering Conference*, 1999.

[15]Ma, X., *Adaptive Extremum Control And Wind Turbine Control*, Ph.D. thesis, Danemark, May 1997.

[16]van der Hooft, E. L., Schaak, P., and van Engelen, T. G., "Wind turbine control algorithms," Ecn windenergie report, Dec. 2003.

[17]Anderson, B. D. O. and Moore, J. B., *Optimal Control*, Prentice-Hall, 1990.

[18]Nijmeijer, H. and Schaft, A. V. D., *Nonlinear Dynamical Control Systems*, Springer-Verlag, 1990.